

CARMENES. I: Instrument and Survey Overview

A. Quirrenbach^a, P. J. Amado^b, W. Seifert^a, M. A. Sánchez Carrasco^b, H. Mandel^a,
J. A. Caballero^c, R. Mundt^d, I. Ribas^e, A. Reiners^f,
M. Abril^b, J. Aceituno^g, F. J. Alonso-Floriano^h, M. Ammler-von Eiffⁱ, G. Anglada-Escudé^f,
R. Antona Jiménez^b, H. Anwand-Heerwart^f, D. Barrado y Navascués^g, S. Becerril^b,
V. J. S. Béjar^j, D. Benítez^g, M. C. Cárdenas^b, A. Claret^b, J. Colomé^e, M. Cortés-Contreras^h,
S. Czesla^k, C. del Burgo^l, M. Doellingerⁱ, R. Dorda^h, S. Dreizler^f, C. Feiz^a, M. Fernández^b,
D. Galadí^g, R. Garrido^b, J. I. González Hernández^j, J. Guàrdia^e, E. W. Guentherⁱ,
E. de Guindos^g, J. Gutiérrez-Soto^b, H.-J. Hagen^k, A. P. Hatzesⁱ, P. H. Hauschildt^k,
J. Helmling^g, T. Henning^d, E. Herrero^e, A. Huber^d, K. F. Huber^k, S. Jeffers^f, V. Joergens^d,
E. de Juan^g, M. Kehrⁱ, A. Klutsch^h, M. Kürster^d, S. Lalitha^k, W. Laun^d, U. Lemke^f,
R. Lenzen^d, J. L. Lizon^m, M. López del Fresno^c, M. López-Morales^e, J. López-Santiago^h,
U. Mall^d, E. L. Martín^c, S. Martín-Ruiz^b, E. Mirabet^b, D. Montes^h, J. C. Morales^e,
R. Morales Muñoz^b, A. Moya^c, V. Naranjo^d, R. Oreiro^b, D. Pérez Medialdea^b, M. Plutoⁱ,
O. Rabaza^b, A. Ramón^b, R. Rebolo^j, S. Reffert^a, P. Rhode^f, H.-W. Rix^d, F. Rodler^e,
E. Rodríguez^b, C. Rodríguez-López^b, E. Rodríguez-Pérez^b, A. Rodríguez Trinidad^b,
R.-R. Rohloff^d, E. Sánchez-Blanco^b, J. Sanz-Forcada^c, S. Schäfer^f, J. Schillerⁱ, C. Schmidt^f,
J. H. M. M. Schmitt^k, E. Solano^c, O. Stahl^a, C. Storz^d, J. Stürmer^a, J. C. Suárez^b, U. Thiele^g,
R.-G. Ulbrich^f, M. Vidal-Dasilva^c, K. Wagner^a, J. Winklerⁱ, W. Xuⁿ, M. R. Zapatero Osorio^c,
and M. Zechmeister^f

^aLandessternwarte, Zentrum für Astronomie der Universität Heidelberg, Königstuhl 12,
D-69117 Heidelberg, Germany;

^bInstituto de Astrofísica de Andalucía (CSIC), Glorieta de la Astronomía s/n, E-18008
Granada, Spain;

^cCentro de Astrobiología (CSIC-INTA), Campus ESAC, PO Box 78, E-28691 Villanueva de la
Cañada, Madrid, Spain;

^dMax-Planck-Institut für Astronomie, Königstuhl 17, D-69117 Heidelberg, Germany;

^eInstitut de Ciències de l'Espai (CSIC-IEEC), Campus UAB, Facultat Ciències, Torre C5 -
parell - 2a planta, E-08193 Bellaterra, Barcelona, Spain;

^fInstitut für Astrophysik (IAG), Friedrich-Hund-Platz 1, D-37077 Göttingen, Germany;

^gCalar Alto Observatory (MPG-CSIC), Centro Astronómico Hispano-Alemán, Jesús Durbán
Remón, 2-2, E-04004 Almería, Spain;

^hDepartamento de Astrofísica, Facultad de Física, Universidad Complutense de Madrid,
E-28040 Madrid, Spain;

ⁱThüringer Landessternwarte Tautenburg, Sternwarte 5, D-07778 Tautenburg, Germany;

^jInstituto de Astrofísica de Canarias, Vía Láctea s/n, E-38205 La Laguna, Tenerife, Spain, and
Dept. Astrofísica, Universidad de La Laguna (ULL), E-38206 La Laguna, Tenerife, Spain;

^kHamburger Sternwarte, Gojenbergsweg 112, D-21029 Hamburg, Germany;

^lUNINOVA-CA3, Campus da Caparica, Quinta da Torre, Monte de Caparica 2825-149,
Caparica, Portugal;

^mEuropean Organisation for Astronomical Research in the Southern Hemisphere,
Karl-Schwarzschild-Str. 2, D-85748 Garching bei München, Germany;

ⁿWenli Xu Optical System Engineering, Kirchenstr. 6, D-74937 Spechbach, Germany

ABSTRACT

CARMENES (Calar Alto high-Resolution search for M dwarfs with Exo-earths with Near-infrared and optical Echelle Spectrographs) is a next-generation instrument for the 3.5 m telescope at the Calar Alto Observatory, built by a consortium of eleven Spanish and German institutions. The CARMENES instrument consists of two separate échelle spectrographs covering the wavelength range from $0.55\ \mu\text{m}$ to $1.7\ \mu\text{m}$ at a spectral resolution of $R = 82,000$, fed by fibers from the Cassegrain focus of the telescope. Both spectrographs are housed in temperature-stabilized vacuum tanks, to enable a long-term 1 m/s radial velocity precision employing a simultaneous calibration with Th-Ne and U-Ne emission line lamps.

CARMENES has been optimized for a search for terrestrial planets in the habitable zones (HZs) of low-mass stars, which may well provide our first chance to study environments capable of supporting the development of life outside the Solar System. With its unique combination of optical and near-infrared échelle spectrographs, CARMENES will provide better sensitivity for the detection of low-mass planets than any comparable instrument, and a powerful tool for discriminating between genuine planet detections and false positives caused by stellar activity. The CARMENES survey will target 300 M dwarfs in the 2014 to 2018 time frame.

Keywords: Spectrographs, Optical Instrumentation, Near-Infrared Instrumentation, Extrasolar Planets, M Dwarfs

1. INTRODUCTION

The discovery and characterization of Earth-like planets with the eventual search for life is, arguably, one of the most exciting scientific endeavors of the coming years. Four centuries after the start of the Copernican revolution, humanity is now at the verge of closing the circle and finding its context in the living Universe. This will undoubtedly have a profound social and scientific impact. The route to this major breakthrough started with the first exoplanet discoveries around Sun-like stars (Mayor & Queloz 1995). Today, nearly 800 exoplanets have been confirmed, and new announcements are arriving at an ever-accelerating pace. Most of the discoveries come from high-precision RV measurements and an increasingly significant number also from photometric transit observations. Parallel progress has been made in the understanding of the properties of these planets, and in particular of their atmospheres, with the identifications of atomic and molecular species. Transit and occultation spectrophotometry in the visible and IR are opening the door to characterizing the physical parameters and chemical compositions of exoplanetary atmospheres. These techniques have already been applied to hot giant planets (e.g., Charbonneau et al. 2002, Tinetti et al. 2007, Knutson et al. 2007, Swain et al. 2010, Sing et al. 2011), hot Neptunes (Stevenson et al. 2010, Beaulieu et al. 2011) and hot super-Earths or mini-Neptunes (Bean et al. 2010, Berta et al. 2012). Even direct detections of planetary molecular absorption lines have been accomplished (Snellen et al. 2010, Rodler et al. 2012).

The progress made to date lays out the basic foundations for the search and characterization of habitable rocky planets. But the way forward into the realm of potentially habitable exoplanets is a challenging one. Rocky planets, those with a well-defined surface and atmosphere and thus potentially hospitable to life, are expected to have masses below $10 M_{\oplus}$ (those planets with masses between 1 and $10 M_{\oplus}$ are dubbed super-Earths). This makes them difficult to detect and further characterize because of the huge contrast (in brightness, mass and projected surface) between the planet and the star (e.g., Mayor & Udry 2008). Considerable attention is focused on the search for true Earth twins, i.e., Earth-like planets around Sun-like stars. In the particular case of radial velocities, detections of low-mass planets and improving statistics have been gathered thanks to the success of the HARPS instrument. A compilation of the results was presented by Mayor et al. (2011) and it shows that low-mass planets ($M < 30 M_{\oplus}$) are extremely abundant (with at least one planet present around $\sim 50\%$ of the stars). Consistent results were obtained by Howard et al. (2012) using the Kepler sample. The information available has already enough statistical significance to yield a quite precise picture of the abundance of planets as a function of mass and orbital period, albeit only up to 50 days or so, i.e., still much shorter than the HZ. And all this is only statistically solid for Solar-type stars. But it is remarkable that less than 20 years of research has shown that planets are ubiquitous in the Universe and probably an integral component of star formation.

Further author information: (Send correspondence to A. Quirrenbach)

A. Quirrenbach: E-mail: A.Quirrenbach@lsw.uni-heidelberg.de, Telephone: +49-6221-541792

The study of M-type stars is gaining momentum as an alternative “fast track” method to discover and possibly characterize hot and temperate rocky exoplanets. M-type stars are the most abundant type of stars in our Galaxy (frequency 70...75%), and therefore obtaining statistics of planet occurrence and architecture around these stars is of great importance for understanding the physics of planet formation and evolution and its dependence on stellar host mass. Planet searches around M-type stars (with masses in the range of 0.1...0.6 M_{\oplus}) have the main advantage of the larger radial velocity signal, the smaller star-planet contrast and the shorter orbital period of the HZ. This has been exploited to find some of the low-mass exoplanets known so far both with radial velocities (Mayor et al. 2009a, Anglada-Escudé et al. 2012) and transits (Charbonneau et al. 2009); although the current number of detections is still low compared with solar analogs. In spite of that, some studies have already been carried out and yield results similar to Sun-like stars but still with poor statistical significance (Bonfils et al. 2011). In particular, the abundance of planets as a function of mass and orbital distance is very loosely constrained, and the much-sought value of η_{\oplus} , i.e., the relative abundance of Earth-type planets in the HZ, still has a 1- σ interval of 0.28 to 0.95. In addition, all the results obtained from RV surveys are only valid for M-type stars of spectral types earlier than M2 or M3. The faintness of the targets and the intrinsic stellar jitter have traditionally limited the investigation of even lower mass stars.

2. THE CARMENES SURVEY

2.1 Scientific Goals

The fundamental scientific objective of the CARMENES project is to carry out a survey of late-type main sequence stars with the goal of detecting low-mass planets in their HZs (see also Quirrenbach et al. 2010). In the focus of the project are very cool stars later than spectral type M4 and moderately active stars. In particular, we aim at being able to detect a 2 M_{\oplus} planet in the HZ of an M5 star. A long-term radial velocity precision of 1 ms^{-1} per measurement will permit to attain such goals. For stars later than \sim M4 ($M < 0.25M_{\odot}$), such precision will yield detections of super-Earths of 5 M_{\oplus} and smaller inside the entire width of the HZ.

We plan to survey a sample of 300 M-type stars for low-mass planet companions. Besides the detection of the individual planets themselves, the ensemble of objects will provide sufficient statistics to assess the overall distribution of planets around M dwarfs: frequency, masses, and orbital parameters. The survey will confirm or falsify the seemingly low occurrence of Jovian planets around M stars, and the frequency of ice giants and terrestrial planets will be established along with their typical separations, eccentricities, multiplicities, and dynamics. Thus, the CARMENES survey can provide the first robust statements about planet formation in the low-mass star regime. The CARMENES sample will be carefully selected to address the distribution of planets in an optimal manner. In this sense, both the detection and non-detection of planets are very relevant results that provide valuable statistical constraints. The successful completion of the CARMENES survey will allow an insightful investigation of planet formation and evolution models, which are still largely unconstrained in the case of low-mass planets around low-mass stars (cf. Alibert et al. 2011).

2.2 Target Selection

Given the expected performance of the two spectrographs, the sample selected for intensive monitoring will be composed of three sub-samples:

- **S1** – 100 stars with $M < 0.25M_{\odot}$ (spectral type M4 and later);
- **S2** – 100 stars with $0.25M_{\odot} < M < 0.30M_{\odot}$ (spectral type M3-M4);
- **S3** – 100 stars with $0.30M_{\odot} < M < 0.60M_{\odot}$ (spectral type M0-M2), relatively bright.

Sample S1 is designed to cover the spectral type domain that can only be studied by CARMENES. Sample S2 is selected to address a pool of targets for which CARMENES is very efficient but comparable to visible spectrographs and will provide a cross-check with other surveys. Sample S3 will have the highest fraction of bright targets and will therefore be best suited as a “poor weather” sample. The brightest stars of all three samples have the potential of providing a sub-sample for the most frequently observed stars for which the detection of low-mass planets should be clearly enhanced. All three samples will necessarily contain a certain

fraction ($\sim 20 - 30\%$) of moderately active stars. This sub-sample of moderately active stars is defined to exploit best the capabilities of CARMENES (i.e. simultaneous coverage of the visible and near-IR), which should allow to disentangle in these stars the effects of activity and exoplanets.

To carry out a proper selection and characterization of the targets, we have created the CARMENCITA database (CARMENES Cool star Information and daTa Archive). The main source of catalog information comes from the Palomar/Michigan State University Survey of nearby stars (PMSU; Reid et al. 1995, Hawley et al. 1996), which contains coordinates, visual magnitudes, distances, proper motions, and spectral indices, such as TiO5, and the H α equivalent width (useful as stellar activity indicator), for 1966 late-type stars. The distances are averaged combinations of Hipparcos trigonometric parallaxes and spectrophotometric determinations, and the spectral types listed are computed from the TiO5 index. This catalog was cross-matched with the 2MASS point source catalog (Cutri et al. 2003) to obtain JHKs magnitudes of each star and then, according to the instrument limiting magnitudes and the observation site, stars with $J > 11.5$ mag and declinations $\delta < -23^\circ$ (zenith distance $> 60^\circ$) were discarded. This sample was completed with new known late-type stars discovered by the Research Consortium on Nearby Stars (RECONS, <http://www.recons.org>) that contain all the known objects up to 10 pc. A few additional late-type stars came from Bochanski et al. (2005) and Irwin et al. (2011). The spectroscopic M dwarf catalog from the SLOAN Digital Sky Survey (West et al. 2011), the new proper motion stars published by Boyd et al. (2011) and the Dwarf Archive maintained by Gelino, Kirkpatrick and Burgasser (<http://dwarfarchives.org>) were also checked for additional potential sample stars. Finally, the stars contained in the catalog by Lépine and Gaidos (2011) are being merged into the CARMENCITA data base.

2.3 Survey Strategy

To obtain the final target sample of 300 objects, we have started an effort to characterize the stars in CARMENCITA with other instrumentation/telescopes accessible to us. These “pre-cleaning” observations involve taking high and low resolution spectra to filter out active stars (i.e., those with strong H α emission), rapid rotators, and binary systems. Furthermore we are conducting adaptive optics and “lucky imaging” observations of all potential targets in order to make sure that there are no close visual companions or background stars within a few arcsec. Any such companion/background star would cause a certain decrease in the RV accuracy, because its scattered light will be variable due to variations in seeing and fiber positioning. We are thus trying to identify and eliminate as many stars as possible that are not suited for high-precision RV work (rapid rotators, close binaries, very active stars, stars with nearby visual companions) before the start of the CARMENES observations.

The initial target list of $\sim 400 \dots 450$ stars will be observed $\sim 5 \dots 10$ times with CARMENES early on for further clean-up and to select a final subset of 300 stars that will constitute the core CARMENES sample. For this core sample we plan to obtain at least 60 measurements per object, and at least 100 measurements for the most interesting systems. The experience gathered with observations in the visible indicates that exoplanets can already be identified with about 30 measurements (Bonfils et al. 2005). However, ~ 100 measurements per object are clearly needed for the detection of a planet with RV semi-amplitude close to the measurement error (e.g., Udry et al. 2007, Mayor et al. 2009a,b), and to discern multiple-planet systems.

It should be emphasized that the very low-mass planets close to the detection limit are the most interesting objects and require most of the measurements. In this scheme, the total number of measurements needed to achieve the goals of our project is:

- 3,500 measurements for sample clean-up of the “pre-cleaned” 400-450 targets (5-10 measurements per object);
- 15,000 additional measurements for 300 targets (for a total of 60 measurements each);
- 4,000 additional measurements for 100 targets (for a total of 100 measurements each).

This yields a grand total of 22,500 measurements.

To observe the sample we will use a typical maximum integration time of 900 s to avoid blurring of the stellar lines because of the Earths diurnal motion, while guaranteeing a S/N value of 150 for targets with $J = 9$. When

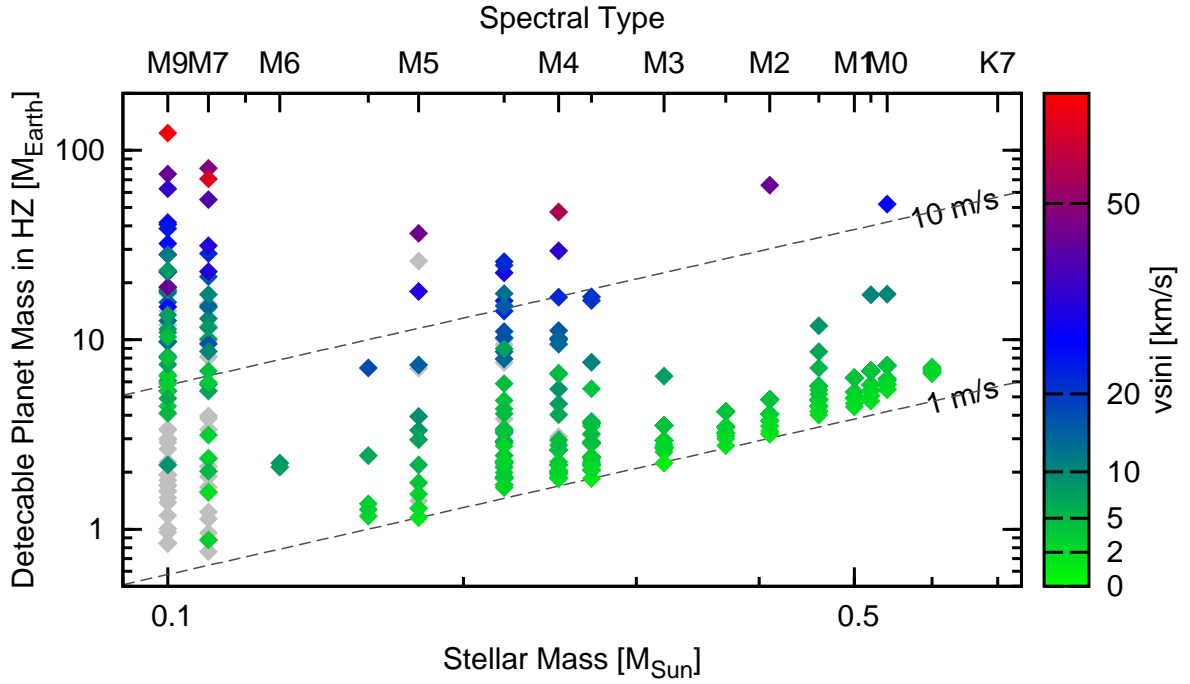


Figure 1. Sample detection limit. The grey diamonds are for $S/N = 150$ in J ; the colored diamonds account for the S/N -limitation of faint stars ($S/N < 150$ for $J < 9$ mag).

considering the expected instrument overheads this leads to an estimate of some 3.5 measurements per hour or some 30 measurements per night. This adds up to 750 clear nights.

2.4 Expected Performance

We have performed simulations of the planet detection capabilities of CARMENES using a preliminary target sample that includes 63 late M dwarfs (M7-M9) presented in Reiners & Basri (2010) and 370 mid and early M dwarfs (M0-M6). For these M dwarfs we have $v \sin i$ values, spectral types, and J magnitudes. From the spectral types of the stars we derived their temperatures and masses. Based on their temperature we assigned highly resolved spectra as provided by new Phoenix models; this allows to estimate the content of RV information. Following Reiners et al. (2010), we calculated the RV precision for each star which is available in each échelle order in the VIS and NIR arms, taking into account the instrumental line broadening, the rotational line broadening, the instrument efficiency (blaze function, gaps, etc.), detector noise, and telluric contamination. For the RV precision calculation, it was assumed that a S/N of 150 in the J band can be achieved with CARMENES within 15 min for stars with $J < 9$ mag. For fainter stars, the photon S/N was rescaled. The S/N in each order depends also on the SED of the stars, which again was derived from the Phoenix model spectra. The total precision σ is obtained by combining the RV measurements of all orders and both arms. From the derived RV precision, we calculated finally detectable masses, assuming that planets can be detected if they induce an RV amplitude K that is equal to the single-measurement precision ($K = \sigma$). The limits for the habitable zones were taken from Kasting et al. (1993).

Figure 1 summarizes the detectable mass in the middle of the habitable zone for all stars studied. For a given stellar mass, the vertical spread is due to the different $v \sin i$ of the stars (color coded). Note that for $S/N = 150$ in J , a total precision of 1 m s^{-1} could be reached for all spectral types. However, for late stars there is a loss of sensitivity mainly due to their faintness (and secondly due to their usually fast rotation). This leads to a minimum of the detectable planet mass at $M = 0.2 M_{\odot}$, suggesting that with CARMENES the lowest-mass planets could be discovered around M dwarfs with spectral types near M5. The goal of being able to detect habitable super-Earths can be attained over a large mass range.

2.5 Calibration

For CARMENES we plan to use hollow cathode lamps for the wavelength calibration. Thorium-Argon and Thorium-Argon-Neon lamps have been used in many other visible-light spectrographs for the same purpose (e.g. HARPS, Mayor et al. 2003). Kerber et al. (2008) have also published a list of 1500 Thorium-Argon-lines in the wavelength regime of the CARMENES near-IR channel. It has been argued, however, that Uranium-Neon lamps have clear advantages in the near-IR, as they provide a higher line density, and suffer less from very bright noble gas lines that are overexposed and contaminate substantial areas on the detector. Since reliable atlases and line lists for these lamps are becoming available (Redman et al. 2011, 2012), we foresee to use Uranium-Neon as a standard calibration source. Our calibration unit design accommodates up to eight different light sources, of which we currently use only five. The remaining three ports can be used for future upgrades (e.g., a laser comb, or a stabilized Fabry-Pérot).

One problem however is that emission line lamps have strong ageing effects. This concerns particularly the Argon lines, which change their position very significantly. Since the ageing depends on how often the lamp is used, it is common practice to install two such lamps. One lamp is used every night, and the other only rarely (master lamp). This means that the lamp that is used every night has to be calibrated against the master lamp on a regular basis. With a typical life time for Thorium-Argon-Neon lamps of 500 hours, the master lamp should not be used for more than 50 hours per year. Given the high short-time stability of CARMENES the cross-calibration can be done by taking spectra with the two lamps sequentially: One frame with one lamp, one frame with the other lamp, one frame with the first lamp and so on. Since we are planning to take about ten such cycles, it is necessary to switch within less than a minute between the two lamps, and the exposure time must be of the order of one minute. The switching between the lamps is done by rotating a mirror in the calibration unit, not by switching on and off the lamps. Thus, during the calibration process both lamps are on, and the rotating mirror selects the light that is fed into the system. The whole cross-calibration between two lamps will take less than one hour. In this way, we will minimize ageing affects of the master lamp, yet obtain enough data to calibrate the lamps against each other.

2.6 Data Reduction

The data reduction will consist of bias, dark, and flat-field corrections, and optimal extraction of the spectrum including the removal of cosmic rays. Flat-fielding will correct for different pixel-to-pixel sensitivity. In addition, a non-linear response of the pixels to different intensity levels will likely have to be corrected for the NIR channel. The necessary calibration frames will be taken every day, and used for the reduction during the following night. A detailed study of the non-linearity of the NIR detectors will need to be carried out before operation, and regular (e.g., quarterly) monitoring is required thereafter. The non-linearity corrections will be implemented in the pipeline based on that data, and updated as necessary based on the regular monitoring.

The radial-velocity measurements will be obtained with the cross-correlation technique using a consistent flux weighting algorithm. Cross-correlation and definition of the center of the cross-correlation profile are standard techniques. We will implement the data analysis package under the same software environment (IDL) as the data reduction package. The wavelength scale for all observed data will be cross-checked over the night and longer time periods. The cross-correlation templates will be binary masks suitable for the range of spectral types that will be observed. Masks can be generated from synthetic spectra, but these models do not always include all relevant lines particularly in the latest spectral types. Therefore, we expect that our cross-correlation masks will evolve during the survey when more and more high-quality spectra are taken, which — at least for the near-IR channel — are currently not available from any other instrument. With a new version of correlation masks, we will re-run the radial velocity analysis for each observation.

The radial-velocity signal will be contaminated by telluric lines, especially in the near-IR. Therefore, spectral regions containing a high density of telluric lines will be ignored in the cross-correlation (and were neglected in our simulations of the RV precision). Other than that, certain features of the stellar spectra can have influence on the RV precision. For example, steep jumps at molecular bands, wide (pressure-broadened) atomic lines, and spectral lines affected by chromospheric emission lines can influence the RV precision in different ways. Since most of our spectral range has not been used for high-precision radial velocity analysis, substantial effort will go into the choice of the optimum wavelength chunks for our analysis. As in the case of the correlation masks,

this optimization can be done when CARMENES is operational, and the full data set can be re-analyzed using improved wavelength chunks.

3. THE CARMENES INSTRUMENT

3.1 Instrument Concept

CARMENES will provide wide wavelength coverage from the visible to the near-IR. This will yield the highest possible precision for the targeted M-type stars while permitting at the same time the discrimination of false-positive RV signals caused by stellar activity. Activity-induced RV variations are expected to be wavelength dependent, which is strictly not the case for orbital variations. The wavelength dependence of activity-induced RV signals will result in at least a factor of 2 to 3 different amplitude in the range 500...1700 nm, and thus provide an efficient and safe way to discard spurious signals (Reiners et al. 2010). The wavelength dependence will also yield valuable information on the spot temperature and distribution. Modeling of light and color curves of cool spotted stars show that near-IR colors (comparing V with I or K fluxes) are more sensitive than visible colors to differences in the spot distribution or structure (two-component spots vs. solid spots, distribution over the surface, etc.). The presence of bright facular components can even produce blue color curves in anti-phase with respect to the near-IR ones (Amado et al. 1999, 2000). The effect of these spot structures on RVs is not yet known but similar differences might be expected, hence the importance of a large wavelength coverage reaching out to the near-IR bands. As a bonus, the high-resolution near-IR data will allow us to study the target stars with unprecedented detail, including their full characterization regarding atmospheric parameters and activity, and possibly carry out powerful diagnostics via asteroseismic analyses.

For late-M spectral types, the wavelength range around 1000 nm (Y band) is the most important wavelength region for RV work (see e.g. Figure 3 in Quirrenbach et al. 2010). Therefore, the efficiency of CARMENES is optimized in this range. Since CCDs do not provide high enough efficiency around 1000 nm and no signal at all beyond the Si cutoff at 1100 nm, a near-IR detector is required. It is thus natural to adopt an instrument concept with two spectrographs, one equipped with a CCD for the range 550-1050 nm, and one with HgCdTe detectors for the range from 0.95-1.7 μm .

Each spectrograph will be coupled to the 3.5 m telescope with its own optical fiber. The front end will contain a dichroic beam splitter and an atmospheric dispersion corrector, to feed the light into the fibers leading to the spectrographs. Guiding is performed with a separate camera. Additional fibers are available for simultaneous injection of light from emission line lamps for RV calibration.

The spectrographs are mounted on benches inside vacuum tanks located in the coudé laboratory of the 3.5 m dome. Each vacuum tank is equipped with a temperature stabilization system capable of keeping the temperature constant to within $\pm 0.01^\circ\text{C}$ over 24 h. The visible-light spectrograph will be operated near room temperature, the NIR spectrograph will be cooled to $\sim 140\text{ K}$.

3.2 Infrared and Visible-Light Spectrographs

The optical design of the spectrographs is based on the FEROS design (Kaufer 1997), being a grism cross-dispersed, white pupil, échelle spectrograph working in quasi-Littrow mode using a two-beam, two-slice, image slicer. The resolving power is 82,000 per sampling element with a mean sampling of 2.8 pix. The peak efficiencies of the instrument, including atmosphere, telescope and fiber link, will be 10% for the visible channel and 13% for the near-IR channel. During the design process, we have tried to keep as much commonality between the two spectrographs as possible.

Each spectrograph consists of a fiber entrance unit (including the image slicer), collimator, échelle grating, cross-disperser grism, camera, and detector unit. These are all described in detail in Seifert et al. (2012), along with the front end that forms the interface to the telescope and contains the acquisition and guiding unit, an atmospheric dispersion compensator (ADC), and the fiber heads.

Since CARMENES uses only the wavelength range up to 1.7 μm , it would be convenient to employ near-IR detectors with a cut-off near that wavelength. Whereas such detectors exist, they have not yet reached the technical and operational maturity of devices with a “standard” 2.5 μm cut-off. It was therefore decided to use

Teledyne HAWAII-2RG detectors with $2.5\ \mu\text{m}$ cut-off, although this necessitates a substantially lower operating temperature for the near-IR spectrograph, in order to keep the thermal background sufficiently low. Detailed calculations concerning this trade-off are presented by Amado et al. (2012).

Both channels need to be extremely stable in terms of their mechanical and thermal behavior; the thermal stability requirement is $\pm 0.07\ \text{K}$ in 24 hours and the goal $\pm 0.01\ \text{K}$. This is achieved by a system that actively cools a shield enclosing the optical bench with the vacuum tank. Thus, the instability produced on the shield temperature is further damped due to the high thermal mass of the optical bench, as well as the high thermal decoupling between both components, the main heat exchange being produced by radiation. The near-IR system employs a separate unit which produces a stable flow of cold nitrogen gas that enters the cooling circuitry of the spectrograph and removes the radiative heat load by means of a group of properly dimensioned heat exchangers. The cooling system is described in detail by Becerril et al. (2012).

3.3 Fibers

Each spectrograph is connected to the front end by two optical fibers with $100\ \mu\text{m}$ core diameter, corresponding to a $1''.5$ diameter field-of-view on the sky. In the default mode, one fiber carries the starlight, while the second fiber is used for simultaneous emission line lamp calibration. Alternatively, the second fiber can be used for sky subtraction.

In slit-coupled spectrographs, guiding errors cause a shift of the spectrum on the detector, leading to spurious radial-velocity variations. This effect is alleviated in fiber-coupled spectrographs such as CARMENES, as the fibers “scramble” the input light: the illumination of the fiber output is more uniform than that of the input. However, standard circular fibers do not remove all spatial information of the incoming flux distribution. This memory is mainly kept in the form of azimuthal symmetry. This effect limits the accuracy of the radial velocity measurement because the point spread function changes with the positioning of the image of the star on the fiber input. This effect can be reduced by an image scrambler consisting of two identical doublets, with the exit pupil of the first fiber system filling exactly the $100\ \mu\text{m}$ core of the second fiber. Alternatively, non-circular fibers (e.g., fibers with square or octagonal core cross section) can provide intrinsically better scrambling as they lack the symmetry that leads to incomplete radial scrambling in circular fibers (e.g., Perruchot et al. 2011). We have tested a classical image scrambler as well as square fibers and find that both can provide the scrambling factor of $\sim 1,000$ required for achieving $1\ \text{m s}^{-1}$ radial velocity precision in CARMENES, with moderate loss of overall throughput. We will likely use square or octagonal fibers as they are more robust and have smaller light losses than classical image scramblers.

3.4 Calibration Unit

The calibration unit contains the lamps that are used for the wavelength-calibration and the flat-fielding. Light from the calibration unit is transmitted to the spectrographs using optical fibers. The stability of the wavelength calibration is of key importance for the accuracy of the radial velocity measurements. There are two sources of errors: One is the motion of the light cone at the entrance of the fiber, the other are changes of spectral line positions produced by the ageing of the lamp. For CARMENES we adopt a design that minimizes both kinds of problems, and provides flexibility for switching between different calibration lamps (see Fig. 2).

Since the typical life-time of a hollow-cathode lamp is 700 to 1000 hours of operation, we will use up one to two lamps per year. Because the wavelength of the emission lines produced by a hollow-cathode-lamps shifts slightly when the lamps gets old, we have to re-calibrate the lamp that is used every day against a light source that is stable in wavelength. However, the ageing of the lamps is mostly due to sputtering by atoms of the cathode when the lamp is on. This means that hollow-cathode lamps do not age much when they are not used. We can thus simply use a lamp that is only rarely used as a master calibration source.

Each calibration unit thus has three master lamps against which the daily lamp can be calibrated. The master lamps will only be used once a week, or 50 to 100 hours per year. The master lamps themselves will thus only age on time scales of years. In order to measure the shift of the master lamps on such time scales, it is planned to calibrate them against three super-master lamps. This has to be done only twice a year. The ageing of the super-master lamps due to sputtering during the lifetime of the CARMENES project will thus be negligible. However, a second ageing effect of hollow-cathode lamps is the exchange of the filling gas of the lamp with the

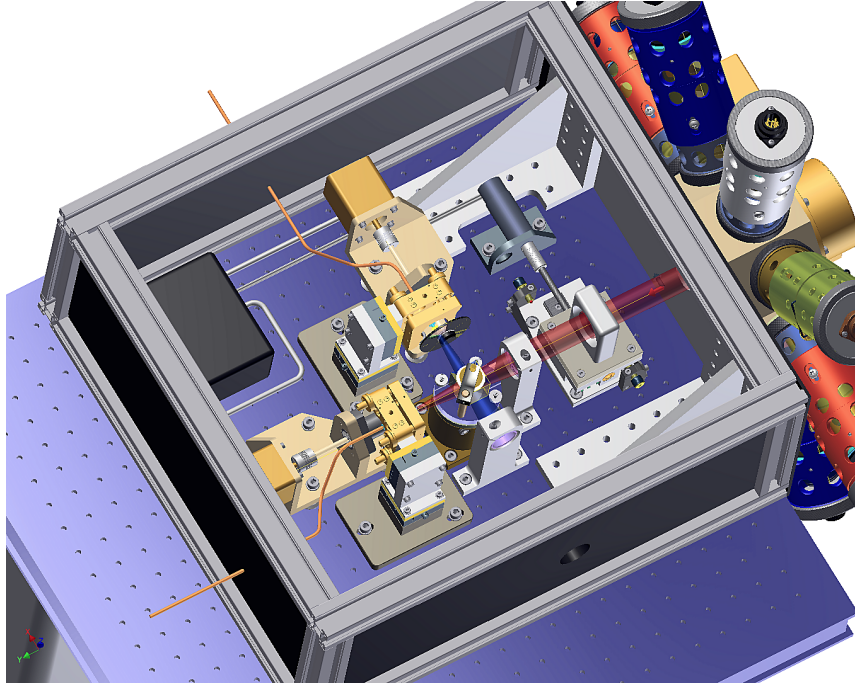


Figure 2. Mechanical Layout of the calibration unit. The emission-line lamps are housed in the cylinders attached to the octagonal structure shown on the right.

outside air. This effect is also present if the lamps are not used. In order to avoid this effect, the super-master lamps are stored in a special container that is filled with the same gas as the lamps. The super-master lamps will only be mounted into the calibration unit when the master lamps are calibrated against the super-master lamps, i.e., only twice a year for a few hours. At all other times, these lamps are in storage. Because we will mount and un-mount the super-master lamps many times during the life time of CARMENES, the super-master lamps are permanently mounted in special protective aluminium rods, and only the aluminium rods will be mounted and un-mounted.

The 8 lamps are mounted on a octagonal structure. Switching between them will be possible in less than one minute simply by rotating a small mirror that sits in the middle of the octagon. A lens in front of the rotating mirror acts as a collimator to parallelize the light. A second lens injects the light into the fiber. Just behind this lens is a beam-splitter cube that splits the light into two parts which then enter the two fibers. If the simultaneous calibration mode is used, only one fiber will be illuminated with light from the calibration unit. This is simply done by closing a rotating shutter in front of one fiber. The light in the other fiber is dimmed down so that exposure times of up to one hour of the lamp are possible. This is done by a circular-variable filter (CVF) in front of the fiber. The CVF allows to dim down the light by a factor of up to 10,000.

3.5 Instrument Control

The coordination and management of the CARMENES instrument is handled by the Instrument Control System (ICS), which is responsible for carrying out the operations of the different subsystems and provides a tool to operate the instrument, with choices from low to high levels of user interaction. The main goals of the ICS and the CARMENES control layer architecture are to maximize the instrument efficiency by reducing time overheads and by operating it in an integrated and efficient manner. An automated scheduler is integrated into the control system architecture. The CARMENES ICS is described in more detail in Guàrdia et al. (2012).

3.6 Environment and Interfaces

The CARMENES instrument will be installed in the coudé room of the 3.5 m telescope (see Fig. 3). The interface with the front end on the telescope is the fiber link that will route the light into the spectrographs. For the

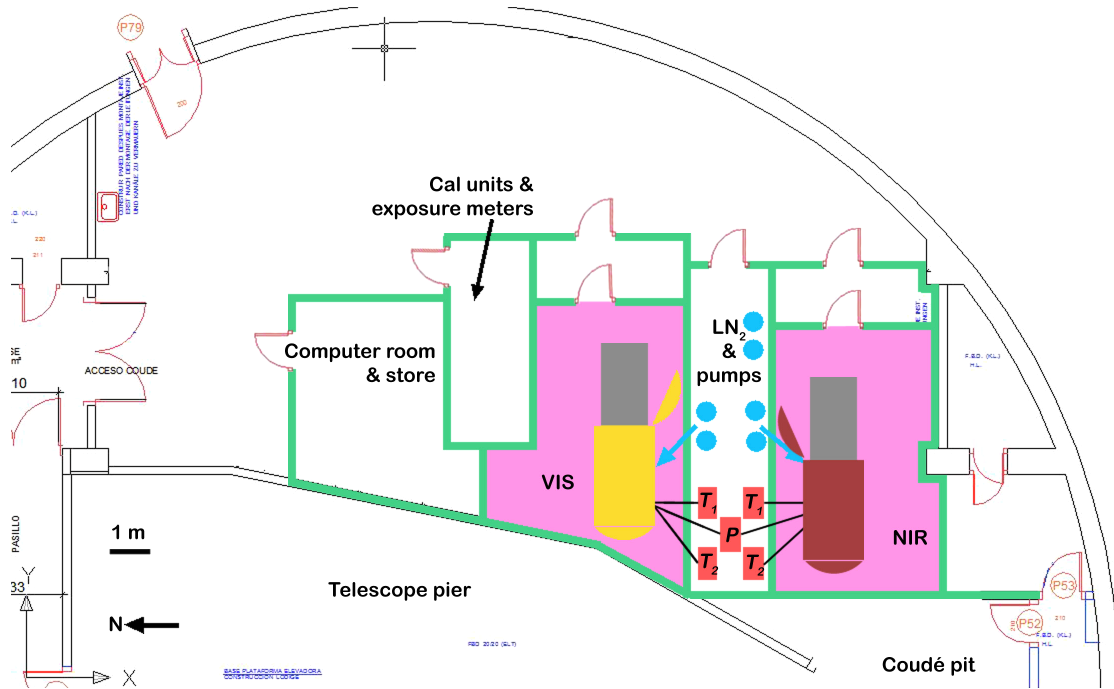


Figure 3. Sketch of the arrangement of the two spectrographs in the coudé laboratory of the 3.5 m telescope. Each spectrograph is located inside a small temperature-controlled room. Service units and electronics are placed outside these rooms as far as possible.

instrument operation, electric power, cooling water, and liquid nitrogen (~ 40 liters per day) are required. These will all routinely be provided by the observatory.

Most spaces in the coudé lab will be simply vented or cooled without a specific stabilization of the temperature. However, the two rooms housing the NIR and VIS vacuum tanks and other devices will be kept at a nearly constant temperature that will be set somewhere between 12 and 15°C . The stability around this mean value will be better than $\pm 1^\circ\text{C}$, as has been verified with temperature sensors installed at several locations within the coudé lab.

4. OUTLOOK

The CARMENES instrument is currently in the final design stage. The final design review of the optical design was held in April 2012, and according to current planning the final design review of the complete instrument will be held in late 2012. Some long-lead items (such as the échelle gratings and the near-infrared detectors) have already been ordered. It is expected that assembly, integration and verification of the spectrographs and other sub-systems will proceed during 2013, followed by commissioning on Calar Alto in the first half of 2014. This will enable us to carry out the CARMENES survey in the 2014 to 2018 time frame.

ACKNOWLEDGMENTS

CARMENES is an instrument for the Centro Astronómico Hispano-Alemán de Calar Alto (CAHA, Almería, Spain). CARMENES is funded by the Max Planck Society (MPG), the Consejo Superior de Investigaciones Científicas (CSIC), and the members of the CARMENES Consortium (see institutions ^a through ^k of the author list), with additional contributions by the Spanish Ministry of Research, the state of Baden-Württemberg, the German Science Foundation (DFG), the Junta de Andalucía, and by the European Union through FEDER/ERF funds.

REFERENCES

1. Alibert, Y., Mordasini, C., & Benz, W. (2011). *Extrasolar planet population synthesis. III. Formation of planets around stars of different masses*. A&A 526, A63
2. Amado, P.J., Butler, C.J., & Byrne, P.B. (1999). *Photometric modelling of starspots - I. A Barnes-Evans-like surface brightness-colour relation using (I_C-K)*. MNRAS 310, 1023-1032
3. Amado, P.J.; Doyle, J.G., & Byrne, P.B. (2000). *Photometric modelling of starspots - II. The FORTRAN code spotpic*. MNRAS 314, 489-497
4. Amado, P.J., Lenzen, R., Cardenas, M.C., Sánchez-Blanco, E., Becerril, S., et al. (2012). *CARMENES: non-cryogenic solutions for YJH-band NIR instruments*. These proceedings, 8450-64
5. Anglada-Escudé, G., Arriagada, P., Vogt, S.S., Rivera, E.J., Butler, R.P., et al. (2012). *A planetary system around the nearby M Dwarf GJ 667 c with at least one super-Earth in its habitable zone*. ApJ 751, L16
6. Bean, J.L., Miller-Ricci Kempton, E., & Homeier, D. (2010). *A ground-based transmission spectrum of the super-Earth exoplanet GJ 1214 b* Nature 468, 669-672
7. Beaulieu, J.P., Tinetti, G., Kipping, D.M., Ribas, I., Barber, R.J., et al. (2011). *Methane in the atmosphere of the transiting hot Neptune GJ 436 b?* ApJ 731, 16
8. Berta, Z.K., Charbonneau, D., Désert, J.M., Miller-Ricci Kempton, E., McCullough, P.R., et al. (2012). *The flat transmission spectrum of the super-Earth GJ 1214 b from Wide Field Camera 3 on the Hubble Space Telescope*. ApJ 747, 35
9. Becerril, S., Lizon, J.L., Sánchez-Carrasco, M.A., Mirabet, E., Amado, P., et al. (2012). *CARMENES (III): an innovative and challenging cooling system for an ultrastable NIR spectrograph*. These proceedings, 8450-168
10. Bochanski, J.J., Hawley, S.L., Reid, I.N., Covey, K.R., West, A.A., et al. (2005). *Spectroscopic survey of M dwarfs within 100 parsecs of the Sun*. AJ 130, 1871-1879
11. Bonfils, X., Delfosse, X., Udry, S., Forveille, T., Mayor, M., et al. (2011). *The HARPS search for southern extra-solar planets XXXI. The M-dwarf sample*. arXiv:1111.5019
12. Bonfils, X., Forveille, T., Delfosse, X., Udry, S., Mayor, M., et al. (2005). *The HARPS search for southern extra-solar planets. VI. A Neptune-mass planet around the nearby M dwarf Gl 581*. A&A 443, L15-L18
13. Boyd, M.R., Winters, J.G., Henry, T.J., Jao, W.C., Finch, C.T., et al. (2011). *The Solar neighborhood. XXV. Discovery of new proper motion stars with $0''.40 \text{ yr}^{-1} > \mu \geq 0''.18 \text{ yr}^{-1}$ between declinations -47° and 00°* . AJ 142, 10
14. Charbonneau, D., Berta, Z.K., Irwin, J., Burke, C.J., Nutzman, P., et al. (2009). *A super-Earth transiting a nearby low-mass star*. Nature 462, 891-894
15. Charbonneau, D., Brown, T.M., Noyes, R.W., & Gilliland, R.L. (2002). *Detection of an extrasolar planet atmosphere*. ApJ 568, 377-384
16. Cutri, R.M., Skrutskie, M.F., van Dyk, S., Beichman, C.A., Carpenter, J.M., et al. (2003). *2MASS All-Sky Catalog of Point Sources*. University of Massachusetts and Infrared Processing and Analysis Center (IPAC/California Institute of Technology)
17. Guàrdia, J., Colomé, J., Ribas, I., Hagen, H.J., Morales, R., et al. (2012). *CARMENES. IV: instrument control software*. These proceedings, 8451-108
18. Hawley, S.L., Gizis, J.E., & Reid, I.N. (1996). *The Palomar/MSU nearby star spectroscopic survey. II. The Southern M dwarfs and investigation of magnetic activity*. AJ 112, 2799-2827
19. Howard, A.W., Marcy, G.W., Bryson, S.T., Jenkins, J.M., Rowe, J.F., et al. (2012). *Planet occurrence within 0.25 AU of Solar-type stars from Kepler*. ApJS 201, 15
20. Irwin, J., Berta, Z.K., Burke, C.J., Charbonneau, D., Nutzman, P., et al. (2011). *On the angular momentum evolution of fully convective stars: Rotation periods for field M-dwarfs from the MEarth transit survey*. ApJ 727, 56
21. Kasting, J.F., Whitmire, D.P., & Reynolds, R.T. (1993). *Habitable zones around main sequence stars*. Icarus 101, 108-128
22. Kaufer, A., Wolf, B., Andersen, J., & Pasquini, L. (1997). *FEROS, the fiber-fed extended range optical spectrograph for the ESO 1.52-m telescope*. The Messenger 89, 1-4

23. Kerber, F., Nave, G., & Sansonetti, C.J. (2008). *The spectrum of Th-Ar hollow cathode lamps in the 691-5804 nm region: establishing wavelength standards for the calibration of infrared spectrographs*. ApJS 178, 374-381
24. Knutson, H.A., Charbonneau, D., Allen, L.E., Fortney, J.J., Agol, E., et al. (2007). *A map of the day-night contrast of the extrasolar planet HD 189733 b*. Nature 447, 183-186
25. Lépine, S., & Gaidos, E. (2011). *An all-sky catalog of bright M dwarfs*. AJ 142, 138
26. Mayor, M., Bonfils, X., Forveille, T., Delfosse, X., Udry, S., et al. (2009a). *The HARPS search for southern extra-solar planets. XVIII. An Earth-mass planet in the GJ581 planetary system*. A&A 507, 487-494
27. Mayor, M., Udry, S., Lovis, C., Pepe, F., Queloz, D., et al. (2009b). *The HARPS search for southern extra-solar planets. XIII. A planetary system with 3 super-Earths (4.2, 6.9, and 9.2 M_⊕)*. A&A 493, 639-644
28. Mayor, M., Marmier, M., Lovis, C., Udry, S., Ségransan, D., et al. (2011). *The HARPS search for southern extra-solar planets XXXIV. Occurrence, mass distribution and orbital properties of super-Earths and Neptune-mass planets*. arXiv:1109.2497
29. Mayor, M., & Queloz, D. (1995). *A Jupiter-mass companion to a solar-type star*. Nature 378, 355-359
30. Mayor, M., & Udry, S. (2008). *The quest for very low-mass planets*. Physica Scripta T130, 014010
31. Mayor, M., Pepe, F., Queloz, D., Bouchy, F., Rupprecht, G., et al. (2003). *Setting new standards with HARPS*. The Messenger 114, 20-24
32. Perruchot, S., Bouchy, F., Chazelas, B., Díaz, R.F., Hébrard, G., et al. (2011). *Higher-precision radial velocity measurements with the SOPHIE spectrograph using octagonal-section fibers*. In *Techniques and instrumentation for detection of exoplanets V*. Ed. Shaklan, S., SPIE Vol. 8151, 815115, p. 1-12
33. Quirrenbach, A., Amado, P.J., Mandel, H., Caballero, J.A., Mundt, R., et al. (2010). *CARMENES: Calar Alto high-Resolution search for M dwarfs with Exo-earths with Near-infrared and optical Echelle Spectrographs*. In *Ground-based and airborne instrumentation for astronomy III*. Eds. McLean, I.S., Ramsay, S.K., & Takami, H., SPIE Vol. 7735, 773513, p. 1-14
34. Redman, S.L., Lawler, J.E., Nave, G., Ramsey, L.W., & Mahadevan, S. (2011). *The infrared spectrum of Uranium hollow cathode lamps from 850 nm to 4000 nm: Wavenumbers and line identifications from Fourier transform spectra*. ApJS 195, 24
35. Redman, S.L., Ycas, G.G., Terrien, R., Mahadevan, S., Ramsey, L.W., et al. (2012). *A high-resolution atlas of Uranium-Neon in the H band*. ApJS 199, 2
36. Reid, I.N., Hawley, S.L., & Gizis, J.E. (1995). *The Palomar/MSU nearby-star spectroscopic survey. I. The Northern M dwarfs – bandstrengths and kinematics*. AJ 110, 1838-1859
37. Reiners, A. & Basri, G. (2010). *A volume-limited sample of 63 M7-M9.5 dwarfs. II. Activity, magnetism, and the fade of the rotation-dominated dynamo*. ApJ 710, 924-935
38. Reiners, A., Bean, J.L., Huber, K.F., Dreizler, S., Seifahrt, A., & Czesla, S. (2010). *Detecting planets around very low mass stars with the radial velocity method*. ApJ 710, 432-443
39. Rodler, F., Lopez-Morales, M., & Ribas, I. (2012). *Weighing the non-transiting hot Jupiter τ Boo b*. ApJ 753, 25
40. Seifert, W., Sanchez-Carrasco, M., Xu, W., Cardenas, C., Sanchez-Blanco, E., et al. (2012). *CARMENES: (II) Optical and Opto-Mechanical Design*. These proceedings, 8446-114
41. Sing, D.K., Désert, J.M., Fortney, J.J., Lecavelier Des Etangs, A., Ballester, G.E., et al. (2011). *Gran Telescopio Canarias OSIRIS transiting exoplanet atmospheric survey: detection of potassium in XO-2b from narrowband spectrophotometry*. A&A 527, A73
42. Snellen, I.A.G., de Kok, R.J., de Mooij, E.J.W., & Albrecht, S. (2010). *The orbital motion, absolute mass and high-altitude winds of exoplanet HD 209458 b*. Nature 465, 1049-1051
43. Stevenson, K.B., Harrington, J., Nymeyer, S., Madhusudhan, N., Seager, S., et al. (2010). *Possible thermo-chemical disequilibrium in the atmosphere of the exoplanet GJ436 b*. Nature 464, 1161-1164
44. Swain, M.R., Deroo, P., Griffith, C.A., Tinetti, G., Thatte, A., et al. (2010). *A ground-based near-infrared emission spectrum of the exoplanet HD 189733 b*. Nature 463, 637-639
45. Tinetti, G., Vidal-Madjar, A., Liang, M.C., Beaulieu, J.P., Yung, Y., et al. (2007). *Water vapour in the atmosphere of a transiting extrasolar planet*. Nature 448, 169-171

46. Udry, S., Bonfils, X., Delfosse, X., Forveille, T., Mayor, M., et al. (2007). *The HARPS search for southern extra-solar planets. XI. Super-Earths (5 and 8 M_{\oplus}) in a 3-planet system.* A&A 469, L43-L47
47. West, A.A., Morgan, D.P., Bochanski, J.J., Andersen, J.M., Bell, K.J., et al. (2011). *The Sloan Digital Sky Survey data release 7 spectroscopic M dwarf catalog. I. Data.* AJ 141, 97